united nations
educational, scientific
and cultural
organization

international atomic
energy agency

the
abdus salam
international centre for theoretical physics

H4.SMR/1202-25

"Fifth Course on Mathematical Ecology
including and introduction to Ecological Economics"

28 February - 24 March 2000

BIOLOCALLY GENERATED SPATIAL PATTERN AND THE COEXISTENCE OF COMPETING SPECIES

Simon Levin

Department of Ecology and Evolutionary Biology
Princeton University
Princeton, NJ
U.S.A.

strada costiera, 11 - 34014 trieste italy - tel. +39 040224011 | fax +39 040224163 - sci_info@ictp.trieste.it - www.ictp.trieste.it

In: (D.Tilman and P.Kareiva, eds.) Spatial Ecology: The Role of Space in Population Synamics and Interspecific Interactions. Princeton University Press, Princeton, NJ. 1997. Pgs. 204-232

CHAPTER NINE

Biologically Generated Spatial Pattern and the Coexistence of Competing Species

Stephen W. Pacala and Simon A. Levin

INTRODUCTION

Simple ecological models typically are designed from the outset either primarily to expose ideas or primarily to describe particular systems. Models in the former category include assumptions that enhance mathematical tractability but make the models more difficult to test. For example, a large class of models in plant ecology relies on the assumption that the habitat is divided into a network of discrete cells with precisely one individual per cell (Skellam 1951; Horn and MacArthur 1972; Shmida and Ellner 1984; Durrett and Levin 1994a,b; Tilman 1994; Pacala and Tilman 1994). The fact that nature lacks this convenient subdivision complicates empirical measurement of quantities in the model and thus limits the model's capacity to scale up practical measurements.

In contrast, models intended to capture particular field systems are easier to estimate but tend to be considerably less tractable than are simple models of ideas. For example, over the past ten years, we and colleagues have developed, estimated, and tested models of plant communities (Pacala and Silander 1985, 1990; Cain et al. 1995; Pacala, Canham, and Silander 1993; Pacala et al. 1996). These models were defined at the level of the single individual simply because short-term data on individual performance are practical to obtain. They include every plant in a large community (10^3–10^6 individuals),

each plant has a unique location, and data-defined submodels predict the fate of each plant throughout its life (birth, dispersal, survivorship, fecundity, and death). Ecological interactions included in the submodels range from the simple spatially local density dependence in neighborhood models (Pacala and Silander 1985, 1990) to the mechanistic (resource-based), and size-structured functions in the SORTIE model of forest dynamics (Pacala et al. 1993, 1996).

The most interesting general result from this body of work is that fine-scale spatial structure is sometimes caused by biological interactions among individuals and that this biologically generated heterogeneity has dramatic effects on dynamics. For each field community studied, it was possible to construct a "mean-field" (see Levin and Pacala, Chapter 12) model with spatially global interactions in place of the local interactions in the calibrated and tested models, thereby eliminating effects of biotic spatial heterogeneity. In cases without significant biotic heterogeneity (an artificially depauperate community of weeds on tilled land), the mean-field model was insignificantly different from the spatial models; both models predicted actual community dynamics and structure in the field (Pacala and Silander 1990). However, in two cases with substantial biotically generated spatial structure, the predictions of the mean-field models deviated sharply both from the spatial models and from nature. In particular, Pacala and Deutschman (1996) showed that the fine-scale spatial structure caused by interactions among individual trees is essential for maintaining both successional diversity and over one-half of the forest's living biomass.

Nonuniform spatial pattern develops in these systems because of relatively short dispersal and short-range interindividual interactions. Long-distance dispersal breaks up nonuniform spatial pattern, and long-range interindividual interactions average over it, causing dynamics to converge to a mean-field limit which can be analyzed and understood (as in the annual community studied by Pacala and Silander 1990).

However, if interactions occur over short distances, then the vital rates of plants may respond dramatically to changes in the local community caused by simple demographic stochasticity (e.g., the response of understory saplings to the death of a

single nearby adult). If dispersal is also short, then the altered local abundances and vital rates will be remembered in the local spatial distribution as further changes in local community composition. In this way, small and unavoidable random fluctuations in the local spatial distribution may become first amplified and then reinserted as larger disruptions of the pattern. Repeated cycles of the process can cause inevitable fine-scale demographic stochasticity to become manifest in large-scale pattern.

Models that include stochastically seeded interplay between spatial structure and dynamics have been so intractable as to preclude even writing down the equations governing average abundances. These nonlinear, spatial stochastic processes have been the province primarily of interesting but difficult and limited theorems (Durrett and Levin 1994a). Paradoxically, our most striking result from a decade of research using data-defined models—the significance of biotic heterogeneity—has been itself the cause of our inability to understand these models fully.

To avoid the problem, most published simple models of ideas either include assumptions that prevent the phenomenon from happening or rely on computer simulations. Some common assumptions that prevent the phenomenon are that dispersal is infinitely large (e.g., Skellam 1951; Horn and MacArthur 1972; Shmida and Ellner 1984; Pacala 1986a,b; Tilman 1994), that the spatial pattern is fixed by some factor outside the model (e.g., the patch models assuming a fixed distribution of individuals per patch such as Atkinson and Shorrocks 1981; Hassell and May 1988; Ives and May 1985), and that the scale of competition is large enough to prevent significant fluctuations in local densities caused by demographic stochasticity (a tacit assumption of mean-field models including virtually all published reaction-diffusion models; see Chapter 12). The limitations of published analytically tractable spatial models are widely acknowledged, however, as evidenced by the large number of recent studies relying on computer simulations of interacting particle systems (including stochastic cellular automata and stochastic point processes, reviewed in Durrett and Levin 1994a,b).

Moment closure methods now offer a way to analyze nonlinear spatial stochastic processes to understand the causes and consequences of biotically generated spatial structure. The method relies on a non-mean-field spatial approximation to write equations governing average abundances of each species (the means or *first moments* of the stochastic process) and equations governing spatial variances and covariances (the second moments). It may be applied to virtually any spatial and stochastic ecological model, including stochastic cellular automata (Durrett and Levin 1994a,b) and point processes such as neighborhood models with finite dispersal (Bolker and Pacala 1997; Pacala 1997). We have even used it to derive equations for the moments of the complex and mechanistic forest simulation model SORTIE (Pacala and Deutschman 1996).

In this chapter we use the moment closure method to analyze some simple models of competition between two species. Our purpose is to introduce some results about the causes and consequences of biotic heterogeneity, to increase the accessibility of the methods, and to illustrate the incompleteness of current theory.

A SIMPLE MODEL OF NEIGHBORHOOD COMPETITION

Consider a community composed of two perennial plant species occupying, for simplicity, a one-dimensional habitat. Mortality is density independent at rate μ_i for species i, and an individual's fecundity, F_i, is a function of the local densities of the two species:

$$F_i(L_i, L_j) = f_i - \beta_i L_i - \alpha_{ij}\beta_i L_j \tag{9.1}$$

where L_i is the local density of conspecifics, L_j is the local density of heterospecifics, f_i is the maximum fecundity rate for species i, β_i governs the effect of conspecific neighbors, and α_{ij} governs the relative strength of inter- and intraspecific interference.

Each individual is located at a point on the line and disperses to its location from its mother with dispersal distance

governed by the Laplacian density (back-to back exponentials):

$$D(x - x_m) = \frac{1}{2M_{D_i}} e^{-(|x - x_m|/M_{D_i})} \qquad (9.2)$$

where x is the position of an offspring, x_m is the position of its mother, and M_{D_i} is the mean dispersal distance for species i. Effects of neighbors on fecundity in Equation 9.1 are assumed to decrease exponentially with distance. To determine the local density of species k ($k = i$ or j) around a species i plant located at position x, one sums the following distance weights over all species k individuals:

$$L_{ik}(x - x_n) = \frac{1}{2M_{C_{ik}}} e^{-(|x - x_n|/M_{C_{ik}})} \qquad (9.3)$$

where x_n is the location of a species k neighbor and $M_{C_{ik}}$ is the spatial scale for the competitive effects of species k neighbors on species i focal plants (analogous to the mean dispersal distance in Equation 9.2).

It is a simple matter to write a computer program that will simulate the dynamics of our two plant species. Beginning with an initial number and spatial distribution and taking Δt to be a very small time interval, one cycles repeatedly through four steps: (1) kill each individual with probability $\mu_i \Delta t$, (2) for each individual, calculate the con- and heterospecific local densities by summing the distance weights (Eq. 9.3), (3) have each individual give birth with probability $\Delta t F_i$, and (4) disperse each new offspring to its new location by drawing a pseudorandom number from the exponential probability density (Eq. 9.2). By cycling repeatedly through these four steps, one can predict the number and spatial distribution of the species at any time in the future.

With the addition of two spatial dimensions (which complicates the discussion below only a little), this model is a serviceable description of the competitive process that does apply to some field systems and can be estimated using simple field experiments (see Pacala 1986b; Pacala and Silander 1990).

However, precisely because of its fidelity to the finite scales of real communities, it is stochastic, nonlinear, and spatial and thus mathematically difficult.

In the limit as either the M_{D_i}'s or M_{C_i}'s tend to infinity, the model becomes mathematically identical to the Lotka-Volterra competition equations. With infinite M_{C_i}'s, the model is a mean-field model because each individual interacts equally with every other individual. The parameters of the Lotka-Volterra equations are then $r_i = f_i - \mu_i$, $r_i/K_i = \beta_i$, with competition coefficients given by the α_{ij} in Equation 9.1.

With infinite M_{D_i}'s but finite M_{C_i}'s, we get a Poisson distribution of individuals. The macroscopic population-level model is then found by calculating the expectation of fecundity times survivorship for a randomly chosen individual. This gives a slightly different set of Lotka-Volterra equations with $r_i = f_i - \mu_i - \beta_i$, and other parameters as before. The difference between the two Lotka-Volterra limits is that in the case of infinite dispersal and finite M_{C_i}'s, neighborhoods are biased by the presence of the focal individual, causing extra within-species density dependence (the extra term of minus β_i in the expression for r_i). The long-dispersal limit is the basis for most previously published analytically tractable neighborhood models (i.e., Pacala and Silander 1985; Pacala 1986a,b), the hawks and doves model with migration on a fast timescale in Chapter 12 (Eq. 9.9; see also Durrett and Levin 1994b), and many discrete-cell models (Skellam 1951; Hastings 1980; Chesson 1983; Shmida and Ellner 1984; Crawley and May 1987; Tilman 1994; Pacala and Tilman 1994).

The long-dispersal limit (with finite scales of competition) yields an average of the right-hand side of the corresponding classical mean-field limit, with the average taken over the Poisson variation in local crowding. It is important to understand that, although the Poisson limit of our simple neighborhood model differs little from the classical mean-field limit, the long-dispersal limit may differ strikingly from mean-field limits if density dependence is nonlinear (e.g., replace Equation 9.1 with an exponential decay; see Pacala and Silander 1985). Hawks and doves coexist in the Poisson limit (Chapter 12), but not in the classical mean-field limit.

Returning to the simple neighborhood model with finite scales, we begin by studying the system experimentally. Typically, the first experiment that one would perform in the field is a removal experiment to measure the strength of interspecific competition. Here we measure competition as it has been measured in literally hundreds of field experiments (see Gurevitch 1992), by removing a small number of individuals of each species in separate plots, and then measuring the resulting changes in population size. Interspecific competition is quantified as the per-capita change following heterospecific removal divided by the per-capita change following conspecific removal. We label this quantity α_{ij}^{CSI}. It is easy to show that the community-level strength of competition, α_{ij}^{CSI}, is equal to the individual-level strength of competition, α_{ij}, in either the mean-field or Poisson limit.

Figure 9.1 shows the results of one set of removal experiments, first reported in Pacala (1997). This example is for the symmetric case in which $f_1 = f_2 = f$, $\mu_1 = \mu_2 = \mu$, $\beta_1 = \beta_2 = \beta$, and $\alpha_{12} = \alpha_{21} = \alpha$, and in which all scales (the M_i's and M_{ij}'s) are equal to M. In each removal experiment, the model was first iterated a hundred time units to approximate equilibrium (on a toroidal habitat one thousand units long). Twenty percent of individuals of one species were then removed at random, and the population size changes were measured over 0.2 further time units. All experiments were replicated nine times.

Note that as expected, α^{CSI} approximately equals α if the scales are large (to produce the triangles shown, every individual interacted equally with every other and dispersal was Poisson). However, with finite scales (circles) α^{CSI} is a *humped function* of α. For α sufficiently close to one, interspecific competition at the community level (α^{CSI}) actually becomes weaker as interspecific competition at the individual level (α) becomes stronger. The parameter values used to produce the circles in Figure 9.1 yield an average of approximately ten to twenty-five important neighbors per-capita (ten to twenty-five individuals within the central 95% of the dispersal and competition functions). Figure 9.2 shows that the effects of finite scales are substantial even with 50–125 important neighbors

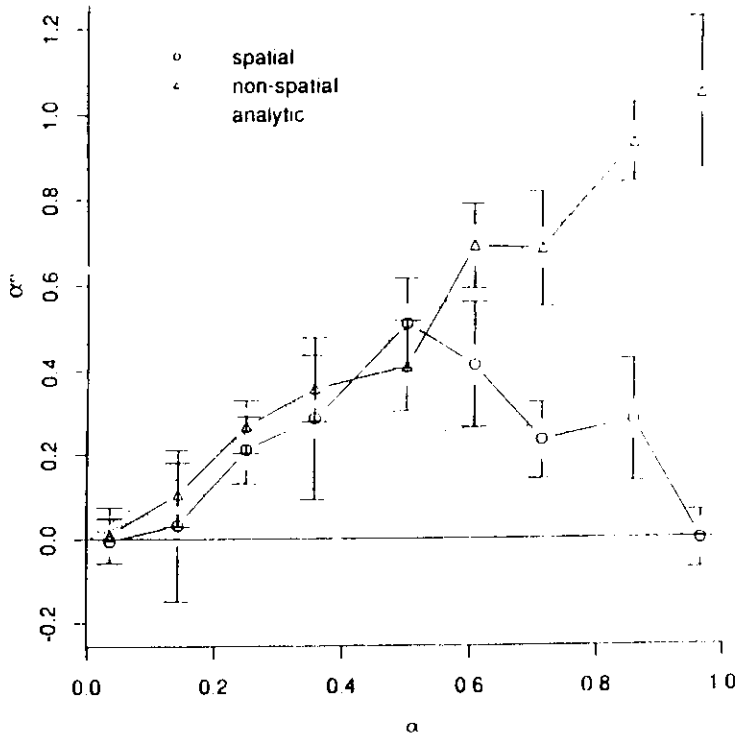

FIGURE 9.1. The strength of interspecific competition (α^{CSI}) as a function of the strength of interindividual interference (α) as determined using removal experiments within the point process. The mean of each of the nine replicates is shown ± one standard deviation. Circles depict runs with $M = 0.2$, and triangles depict runs with spatially global competition and infinite dispersal (Poisson scatter of offspring). The smooth curve is a plot of Equation 9.13. Parameter values were $\Delta t = 0.1$, $f = 3.2$, $\beta = 0.28$, $\mu = 0.4$, $M = 0.2$, and the habitat was a thousand units long.

per plant ($M = 1$) and that the strength of competition decreases as M decreases. Moreover, the α–α^{CSI} relationship appears to be humped for all finite values of M. For example, a run with $M = 5$ and $\alpha = 0.99$ (approximately three hundred important neighbors per plant on average) produced an actual strength of competition of only 0.04.

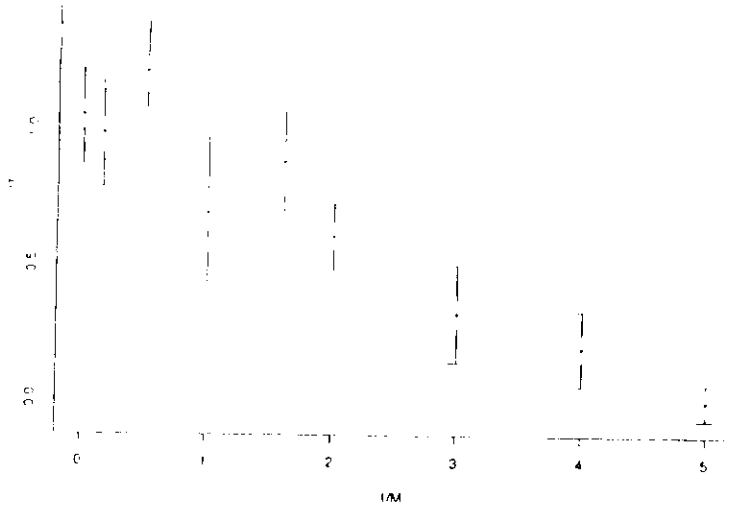

FIGURE 9.2. The strength of interspecific competition ($\alpha^{(M)}$) as a function of the scales of competition and dispersal (M). The horizontal axis gives the reciprocal of M. Parameter values were as in Figure 9.1, but with $\alpha = 0.96$.

The results in Figures 9.1–9.2 leave us with a series of questions. Why are these counterintuitive results obtained? What eliminates competition as the species become identical (as α approaches 1)? Are these phenomena important in real ecosystems? Why are the mean-field and Poisson limits that dominate the theoretical literature so misleading and incomplete? The answers lie in the interplay between stochastically seeded spatial structure and dynamics.

MOMENT CLOSURE

A Pseudospatial Model

Before turning to the analysis of the point process itself, we first consider a simpler system that shares its locally stochastic dynamics. We make two changes in the point process. First, the environment is divided into a gridwork of identical cells, and

the local densities that affect fecundity (the L's in Equation 9.1) are simply the within-cell densities. Second, when an offspring of species i is produced, it stays within its mother's cell with probability m_i and moves to a randomly chosen cell with probability $1 - m_i$ (as in many discrete-cell models such as Shmida and Ellner 1984 and Pacala and Tilman 1994). These changes to the point process impose both a patch structure that obviates information about within-patch locations and a dispersal pattern that obviates information about the spatial arrangement of patches.

Let $P(n_1, n_2)$ be the probability at time t that a randomly chosen patch contains n_1 individuals of species 1 and n_2 individuals of species 2. The probability that a patch containing n_i individuals of species i loses an individual during the small time interval Δt is simply the probability that one of the n_i individuals dies: $\mu_i n_i \Delta t$. Similarly, the probability that the patch gains an individual is the probability that an individual is born within the patch and does not disperse: $(f_i - \beta_i n_i - \alpha_{ij}\beta_i n_j)n_i \Delta t(1 - m_i) = F_i(n_i, n_j)\Delta t(1 - m_i)$, plus the probability that a recruit disperses into the patch from outside it:

$$\overline{n_i F_i}\,\Delta t\, m_i \equiv \sum_{n_1=0}^{\infty} \sum_{n_2=0}^{\infty} P(n_1, n_2) n_i F_i(n_1, n_2)\,\Delta t\, m_i. \quad (9.4)$$

The above expression is simply the mean production of new species i across all patches, times the probability of dispersal.

With these definitions, we may write an expression for temporal changes in the probability distribution $P(n_1, n_2)$:

$$\begin{aligned}\frac{dP(n_1, n_2)}{dt} = &-P(n_1, n_2)\Big[n_1 F_1(n_1, n_2)(1 - m_1) \\ &+ n_2 F_2(n_1, n_2)(1 - m_2) \\ &+ \mu_1 n_1 + \mu_2 n_2 + \overline{n_1 F_1} m_1 + \overline{n_2 F_2} m_2\Big] \\ &+ P(n_1 - 1, n_2)\Big[(n_1 - 1)F_1(n_1 - 1, n_2)\end{aligned}$$

$$\times (1 - m_1) + \overline{n_1 F_1} m_1 \Big]$$

$$+ P(n_1, n_2 - 1)\Big[(n_2 - 1)F_2(n_1, n_2 - 1)$$

$$\times (1 - m_2) + \overline{n_2 F_2} m_2 \Big]$$

$$+ P(n_1 + 1, n_2)(n_1 + 1)\mu_1$$

$$+ P(n_1, n_2 + 1)(n_2 + 1)\mu_2. \qquad (9.5)$$

The problem with the system Equation 9.5 is that it describes an infinite number of equations, one for every possible combination of n_1 and n_2. We seek a simpler system that includes only some of the information in Equation 9.5.

Let N_i be the average abundance of species i across the habitat (mean number per patch). The first equation in Equation 9.6 governs the dynamics of the first moment, N_i (see the Appendix for its derivation):

$$\frac{dN_i}{dt} = N_i\left[f_i - \mu_i - \beta_i\left(N_i + \frac{\sigma_i^2}{N_i}\right) - \alpha_{ij}\beta_i\left(N_j + \frac{C}{N_i}\right)\right]$$

$$\frac{d\sigma_i^2}{dt} = \frac{dN_i}{dt} - 2\mu_i(\sigma_i^2 - N_i)$$

$$+ 2\sigma_i^2(1 - m_i)[f_i - 2\beta_i N_i - \alpha_{ij}\beta_i N_j]$$

$$- 2\alpha_{ij}\beta_i(1 - m_i)N_i C \quad (i, j) = (1, 2), (2, 1)$$

$$\frac{dC}{dt} = C[-(\mu_1 + \mu_2)$$

$$+ (1 - m_1)F_1(N_1, N_2) + (1 - m_2)F_2(N_2, N_1)]$$

$$- \alpha_{21}\beta_2(1 - m_2)N_2\sigma_1^2 - \alpha_{12}\beta_1(1 - m_1)N_1\sigma_2^2. \qquad (9.6)$$

The problem with this equation is that it depends on second moments, σ_i^2 and C, as well as on the first moments N_1 and

N_2. These second moments are σ_i^2, the variance from patch to patch in the abundance of species i, and C, the corresponding covariance between the abundances of the two species.

$$C = \sum_{n_1=0}^{\infty}\sum_{n_2=0}^{\infty}(n_1 - N_1)(n_2 - N_2)P(n_1, n_2)$$

$$= \sum_{n_1=0}^{\infty}\sum_{n_2=0}^{\infty} n_1 n_2 P(n_1, n_2) - N_1 N_2.$$

Third moments are defined as

$$\sum_{n_1=0}^{\infty}\sum_{n_2=0}^{\infty}(n_i - N_i)(n_j - N_j)(n_k - N_k)P(n_1, n_2)$$

where i, j, and k may be equal to one or two in any combination (i.e., $i = 1$, $j = 1$, $k = 2$), and so on to fourth and higher moments. Although in this case the equations for the means depend only on the first two moments, in other cases higher moments will also be involved. The reason that third and higher moments do not arise in the equations for the means in Equation 9.6 is that the density-dependent functions (the F_i's) are linear; higher moments would result with nonlinear functions.

The second moments in the first equation in Equation 9.6 account for the effects of biologically generated spatial structure. The term $N_i + \sigma_i^2/N_i$ is the mean local density of conspecifics in the patch of a randomly chosen individual of species i (rather than in a randomly chosen patch). The mean local density grows with the between-patch variance, σ_i^2, because increasing numbers of individuals are located in clusters as σ_i^2 increases. Similarly, $N_j + C/N_i$ is the mean local density of heterospecifics in the patch of a randomly chosen species i. This density is elevated above the global mean, N_j, if the two species are spatially aggregated ($C > 0$) and depressed beneath it if the species are spatially segregated ($C < 0$). Note that if both the variance and covariance are equal to zero, then the

first equation in Equations 9.6 is identical to the classical mean-field limits, whereas if the spatial distribution is Poisson ($\sigma_i^2 = N_i$ and $C = 0$), the first equation is identical to the long-dispersal limit.

The equations for the means, N_1 and N_2, do not constitute a closed system of equations, because the variances and covariances are themselves full state variables that will change through time because of local interactions and finite dispersal. To close the system, we require the equations governing the dynamics of σ_1^2, σ_2^2, and C. This illustrates the difference between Equations 9.5 and 9.6 and the kind of spatial models that dominate the theoretical literature. Simply adding diffusion terms to equations governing mean densities is not sufficient to describe stochastic processes with local interactions and finite dispersal.

In the Appendix we derive the equations governing the variances and covariances. These equations contain third moments. Because the third moments are again state variables, the equations governing the first two moments do not constitute a closed system. This illustrates the crux of the problem: Any system of equations governing the first n moments contains yet higher moments. What is needed is some closure rule that either states that some moments are negligible or expresses the higher moments in terms of lower moments.

Here we adopt the simplest closure rule. In the Appendix we show that the terms containing the third moments in the equations for the variances and covariances are negligible if both mean numbers of individuals per patch and movement rates are not too small. By omitting these negligible terms, we arrive at the approximate and closed system in Equations 9.6.

The accuracy of the approximation 9.6 is assessed simply by comparing the moments predicted by Equations 9.5 and 9.6 (Figures 9.3 and 9.4). For example, consider the symmetric case used to produce Figures 9.1–9.2 (with equal f's, μ's, β's, α's, and m's). The relationship between the community- and individual-level strengths of competition predicted by approximation 9.6 is a close approximation of the relationship predicted by the actual system (Eq. 9.5) in most cases (Figure 9.3).

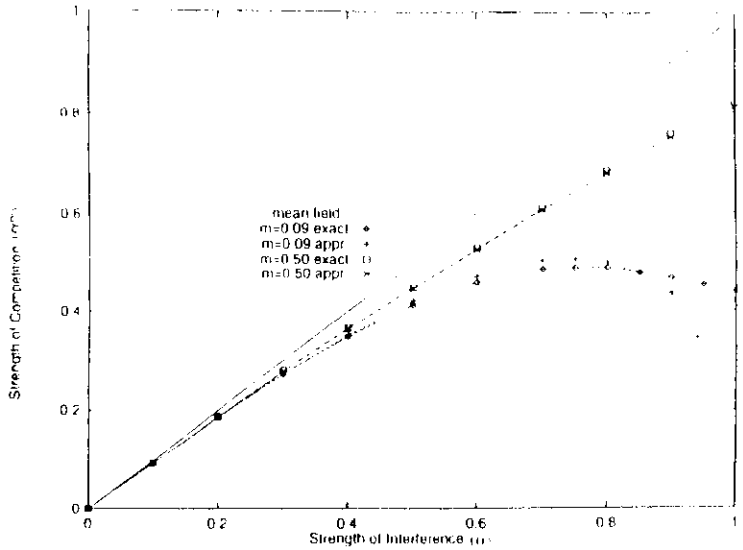

FIGURE 9.3. Equation 9.7 as predicted by the pseudospatial model (Eq. 9.5) (labeled exact) and the moment Equations 9.6 (labeled appr.). The value from the moment equations with $\alpha = 1.0$ and $m = 0.09$ is missing because the equations failed to converge for this set of parameter values. Other parameters were $f = 2.2$, $\mu = 0.88$, and $\beta = 0.066$.

The approximation fails with small m and α close to one because stochastic drift of the relative abundances within each patch is then large, and this leads to large third moments (because most patches contain primarily either species 1 or species 2).

Note that the α–α^{est} relationship given by Equations 9.5 and 9.6 may be humped, but only if the movement rate m is small. In contrast, our numerical work suggests that the relationship is humped in the point process for any finite value of M (as in Figure 9.1).

Because of the analytically tractable approximation (9.6), we are now in a position to explain the occurrence of an inverse relationship between α and α^{est}. Using the first equation in Equation 9.6, it is easy to show for a small number of

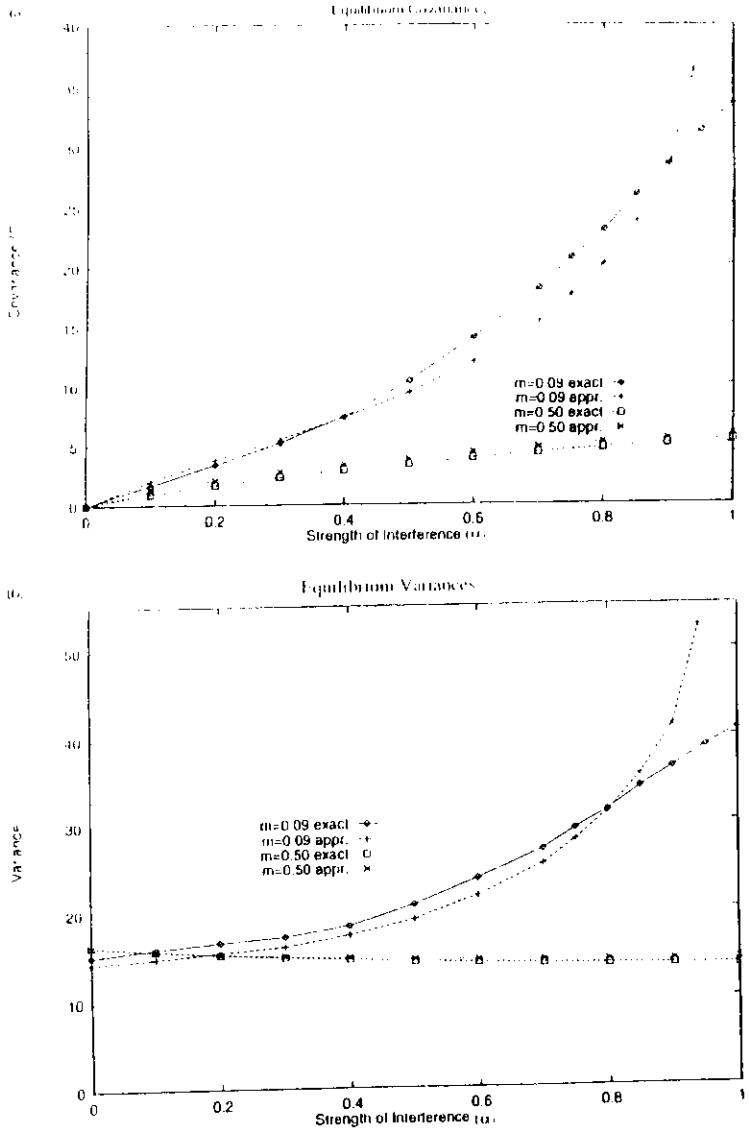

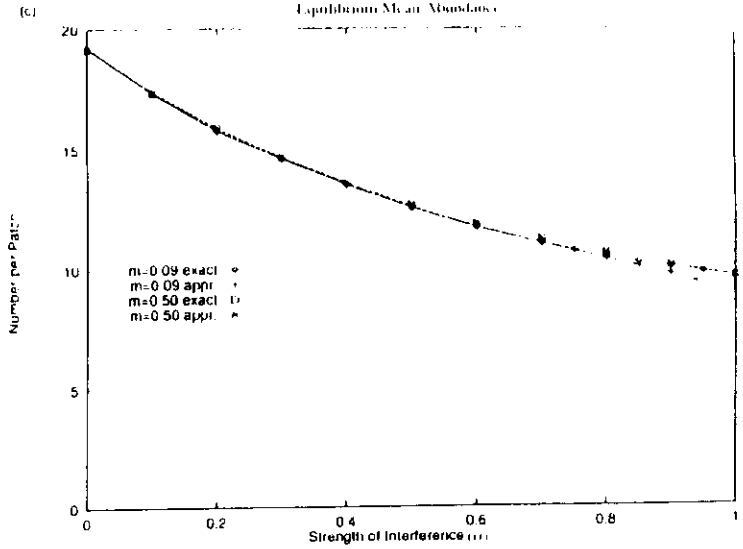

FIGURE 9.4. The moments at equilibrium predicted by the pseudospatial model (Eq. 9.5) (labeled exact) and the moment Equations 9.6 (labeled appr.). Parameter values were as in Figure 9.4. (a) Equilibrium interspecific covariance. (b) Equilibrium intraspecific variance. (c) Equilibrium means.

individuals removed in the removal experiment that

$$\alpha^{est} \approx \alpha \left[\frac{1 + \hat{C}/\hat{N}^2}{1 + \hat{\sigma}^2/\hat{N}^2} \right] \tag{9.7}$$

where the hats above the moments signify equilibrium; α^{est} is depressed beneath α because the spatial covariance is negative at equilibrium. Negative covariance implies interspecific spatial segregation. If covariance is sufficiently negative, then each patch contains primarily only one of the two species. The cause of the spontaneous spatial segregation in the model is a process directly analogous to genetic drift, which removes genetic polymorphism in small populations. Local populations in the models are kept small by density dependence, allowing

relatively large random fluctuations in local relative abundance (demographic stochasticity). The random "drift" of either species toward high local relative abundance is reinforced by local dispersal, which biases the community composition of new recruits in favor of the locally most abundant species.

Note that the degree of the spatial segregation predicted by the pseudospatial model at equilibrium (the covariance in Eq. 9.7) increases as dispersive coupling decreases (Figure 9.4a). This explains the corresponding result in Figure 9.2 from the point process. Again, local dispersal facilitates local "ecological drift." The segregation also increases as interspecific competition at the individual level strengthens (Figure 9.4a) because the deterministic forces opposing drift toward local monodominance decrease in strength as α approaches one. A hump in the relationship between α and α^{CSI} occurs when the increasing spatial segregation overwhelms the increasing strength of individual-level competition.

Changes in m and α also affect α^{CSI} through changes in the variances (see Eq. 9.7). These changes generally complement those described above; within-species spatial aggregation (variance to mean ratio greater than one) develops to accompany the between-species segregation (Figure 9.4b). However, the effect of the variance is complicated by the fact that with small α, increased coupling may either increase clustering ($\sigma^2 > N$) or overdispersion ($\sigma^2 < N$) depending on the values of f, β, and μ.

It is possible to derive from Equation 9.6 useful simple formulae for the spatial moments at equilibrium. For example, if equilibrium population sizes are large and m is close to one then the covariance at equilibrium is approximately

$$\hat{C} \approx -\hat{N}_1\hat{N}_2(1 - m)\frac{\alpha\beta}{\mu} \tag{9.8}$$

and α^{CSI} is approximately

$$\alpha^{CSI} \approx \alpha\left[1 - (1 - m)\alpha\frac{\beta}{\mu}\right]. \tag{9.9}$$

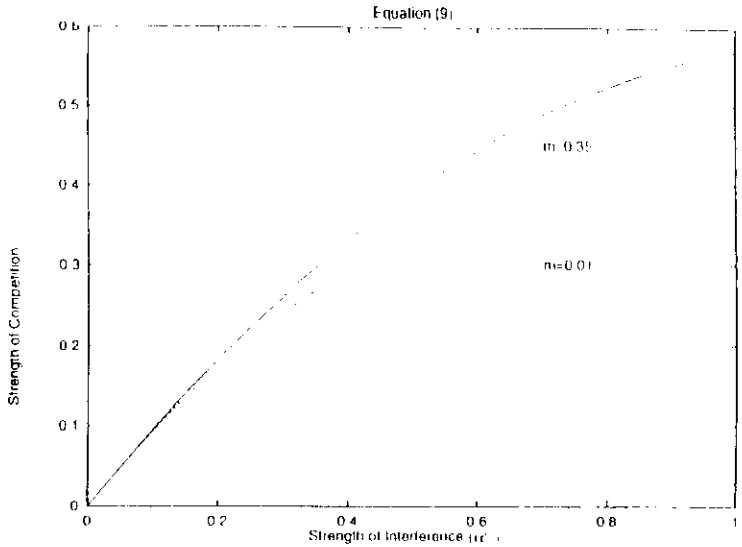

FIGURE 9.5 Equation 9.9 with $\beta/\mu = 0.67$.

Note that α^{CSI} is a humped function of α, but that the hump can occur for α between zero and one only if m is sufficiently small (and $\beta/\mu > 0.5$, Figure 9.5).

Finally, although we do not have the space to treat this subject fully, the model 9.5–9.6 also predicts new and unexplored mechanisms of coexistence. For example, Figure 9.6 shows an interesting case in which the two species are unable to coexist in either the mean-field or Poisson limits because $\alpha_{12} = \alpha_{21} = 1$. In either of these limits, species 2 is the superior competitor, but species 1 has a higher population growth rate in uncrowded conditions. Species 1 is weedy, with early successional vital rates, whereas species 2 has late-successional vital rates. It is easy to construct a simple submodel of resource competition to show that species 2 has the lowest R^* (*sensu* Tilman 1982). Note that the two species coexist if we give species 1 the more rapid dispersal to complement its weedy vital rates (Figure 9.6, $m_1 = 0.9$ and $m_2 = 0.5$). However, there is more happening here than a simple competition-colonization trade-off. Note that if we increase m_1 still further

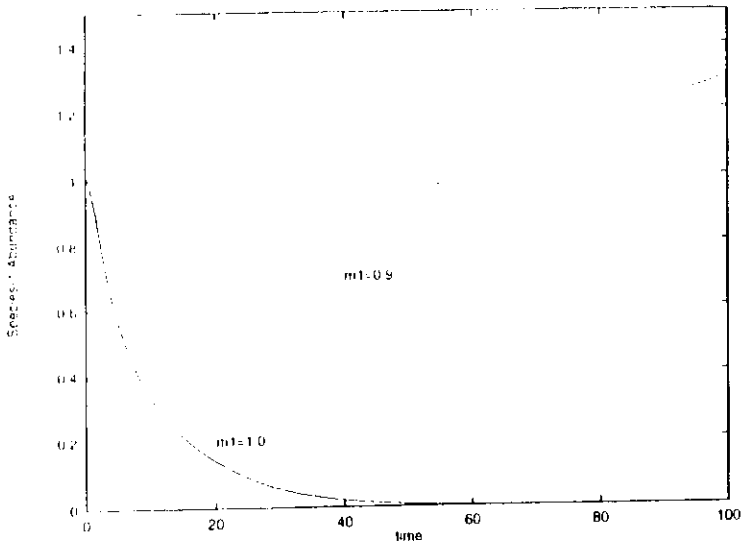

FIGURE 9.6. Two runs of the pseudospatial model (Eq. 9.5) in which species 1 competed against an equilibrium monoculture of species 2. Invasion succeeded if $m_1 = 0.9$ but failed if $m_1 = 1.0$. Other parameter values include $f_1 = 2.2$, $\mu_1 = 0.20$, $\beta_1 = 0.2$, $f_2 = 1.05$, $\mu_2 = 0.8$, $\beta_2 = 0.02$, $m_2 = 0.2$, and $\alpha_{12} = \alpha_{21} = 1$. With these parameter values, species 2 had a larger equilibrium in monoculture than species 1 with either $m_1 = 1.0$ or $m_1 = 0.9$.

to 1.0, then species 1 goes extinct (Figure 9.6). If m_1 is too large, then species 1 cannot develop the degree of spatial segregation it requires to coexist with species 2.

For simplicity, we now restrict our attention to the simplest case, involving the smallest possible perturbation of the long-dispersal (Poisson) limit. We assume that $m_2 = 1$ so that species 2 always has a Poisson distribution and that m_1 is only slightly less than one. We further stack the deck against interesting behavior by assuming that $\alpha_{12} = \alpha_{21} = 1$. This eliminates the coexistence and founder control in both the Poisson and mean-field limits.

The assumption that $m_2 = 1$ and m_1 is near one ensures that spatial aggregation and segregation in the model will be small. Thus, to observe the effects of space, we must correspondingly

weaken the nonspatial forces in the model. Let λ_{pi} be the eigenvalue governing the invasion of species i in an equilibrium monoculture of species j in the Poisson case ($m_1 = m_2 = 1$). It is easy to show that $\lambda_{pi} = f_i - \mu_i - \beta_i(f_j - \mu_j)/\beta_j$. We assume that both λ_{p1} and λ_{p2} are near zero, indicating near-competitive equivalence in the Poisson limit (e.g., $(f_1 - \mu_1)/\beta_1$ is close to $(f_2 - \mu_2)/\beta_2$).

Returning to the case in which $m_1 < 1$, species 1 can invade an equilibrium monoculture of species 2 (first condition below), and species 2 can invade an equilibrium monoculture of species 1 (second condition) if

$$0 < \lambda_{p1} + (1 - m_1)\beta_1(S - A)$$

$$0 < \lambda_{p2} + (1 - m_1)\beta_2\left(A - S\frac{\mu_2}{\mu_1}\right) \qquad (9.10)$$

where $S = \beta_1((f_2 - \mu_2)/\beta_2 - 1)/(\mu_1 + \mu_2)$ and $A = 1 + \beta_1/\mu_1$. Condition 9.10 is derived using a standard local stability analysis, assuming that $\alpha_{12} = \alpha_{21} = m_2 = 1$, and omitting all terms of order $(1 - m_1)^2$, λ_{p1}^2, λ_{p2}^2, $\lambda_{p1}\lambda_{p2}$, $\lambda_{pi}(1 - m_1)$, $\lambda_{pi}(1 - m_1)$ or higher.

The quantities S and A are easily interpretable as spatial effects. Quantity S describes the buildup of spatial segregation during invasion. To see this, replace dC/dt in the last equation in Equations 9.6 by zero and solve for the equilibrium covariance $C(N_1, N_2)^*$. Then divide $C(N_1, N_2)^*$ by N_1, and set N_2 equal to the monoculture equilibrium for species 2 ($N_2^* = (f_2 - \mu_2)/\beta_2 - 1$):

$$\lim_{N_1 \to 0} \frac{C(N_1, N_2^*)}{N_1} = -S(1 - m_1). \qquad (9.11)$$

Thus, S quantifies how spatial segregation grows relative to the mean during invasion.

Similarly, A describes the buildup of intraspecific aggregation by species 1 during invasion (species 2 cannot aggregate because $m_2 = 1$). Replacing $d\sigma_1^2/dt$ with zero in Equations 9.6 and solving for the equilibrium variance $\sigma_1^2(N_1, N_2)^*$, we find

that

$$\lim_{N_1 \to 0} = \left[\frac{\sigma_1^2(N_1, N_2^*)}{N_1} - 1 \right] = A(1 - m_1).$$

If A is positive, then species 1 clusters as it invades because σ_1^2 grows faster than N_1. In contrast, if A is negative, then species 1 becomes evenly dispersed as it invades. Putting all this together, we see from Equation 9.10 that species 1 will invade if interspecific segregation grows sufficiently faster than aggregation and will fail to invade if aggregation grows sufficiently faster than segregation.

To expose only the spatial effects, it is convenient to consider the further restriction that $\lambda_{p1} = \lambda_{p2} = 0$. Then, the two species will coexist if $1 < S/A < \mu_1/\mu_2$; species 1 will invariably exclude species 2 if $1 < S/A$ and $\mu_1/\mu_2 < S/A$; species 2 will exclude species 1 if $1 > S/A$ and $\mu_1/\mu_2 < S/A$; and founder control will result if $\mu_1/\mu_2 < S/A < 1$. We have checked all of these outcomes both in the exact system 9.5 and in the approximation 9.6; spatial effects alone are capable of producing any of the four different outcomes of competition.

Two primary conclusions emerge from the stability analysis. First, long dispersal is not always beneficial. It facilitates persistence if the tendency to segregate is larger than the tendency to cluster but impedes persistence otherwise. Second, the interplay of local competition and dynamics is dynamically rich; it has the potential to transform any of the four quantitatively different outcomes of competition in the Poisson or mean-field limits (coexistence, founder control, exclusion of species 1, or exclusion of species 2) into any other outcome.

The Point Process

We now return to the point process that produced Figures 9.1–9.3. The point process is more difficult than the pseudospatial model above because there is no simple expression analogous to Equation 9.5. However, we can proceed directly to the moment approximations analogous to Equations 9.6.

Bolker and Pacala (1997) show that the equation for the mean abundance of species i in the point process converges to the first equation in Equations 9.6 with

$$\sigma_i^2 = U_{ii}(0)N_i + \int_{y \neq 0} U_{ii}(y)c_{ii}(y)\,dy, \qquad C = \int U_{ij}c_{ij}(y)\,dy \tag{9.12}$$

where the U's are given by Equation 9.3. The function $c_{ij}(y)$ is the interspecific spatial covariance function. Consider many pairs of small quadrates of area A, with the members of each pair a distance y apart. The expected covariance between the *densities* of species 1 in one member of a pair and species 2 in the other is $c_{ij}(y)$ in the limit of small A. Similarly, $c_{ii}(y)$ gives the within-species spatial covariance.

To complete the model, Bolker and Pacala (1997) derived integro-partial differential equations for the dynamics of $c_{11}(y)$, $c_{22}(y)$, and $c_{12}(y)$. During the derivation, they closed the system by assuming that all third central moments were zero, exactly as in the derivation of Equations 9.6 (Bolker and Pacala 1997).

Pacala (1997) reported an equation for α^{est}, obtained by solving for the equilibrium values of N_1, N_2, $c_{11}(y)$, $c_{22}(y)$, and $c_{12}(y)$:

$$\alpha^{\text{est}} = \alpha\left(\frac{M\sqrt{1-\alpha} - W}{M\sqrt{1-\alpha} + W}\right), \qquad W = \frac{\beta}{f-u}\sqrt{\frac{2\mu}{f-u}}. \tag{9.13}$$

For simplicity, this expression is presented for the special case in which M is relatively large and α is close to one. The fact that α^{est} in Equation 9.13 may be negative for very small M is an artifact of this approximation. However, the plot in Figure 9.1 shows that Equation 9.13 generally provides a reasonably accurate approximation (note that M is relatively small in Figure 9.1).

Unlike the pseudospatial system (Eqs. 9.5–9.6), but consistent with the simulations of the point process, expression 9.13

predicts that the α–α^{CSI} relationship is humped even for large values of M. Note in expression 9.13 that the hump will always occur at a value of α between zero and one, with the hump closer to one the larger the ecological scales M.

The difference between the pseudospatial model and the point process is explained by the between-species covariance (recall expression 9.7). In the same case leading to equation 9.13

$$\hat{c}_{12}(x) \approx -\frac{\hat{N}}{2M\sqrt{(1-\alpha)\hat{N}/\mu}}\, e^{-\sqrt{(1-\alpha)\hat{N}/\mu}}. \quad (9.14)$$

Because of the $1 - \alpha$ term in the denominator of Equation 9.14, the interspecific spatial covariance becomes strongly negative as α approaches one. This implies that the two species spontaneously segregate into large monospecific patches in the point process if α is close to one (even if M is large), thereby causing the observed drop in α^{CSI} toward zero (Figure 9.1). The phenomenon is similar to the spatial clustering exhibited by some discrete interacting particle systems, such as the voter model (Durett and Levin 1994a).

The difference between the pseudospatial model and the point process is that extreme levels of spatial segregation occur only at very low levels of coupling (small m) in the pseudospatial model, but at large or small ecological scales (M) if α is near one in the point process (compare expressions 9.8 and 9.13). Because the spatial distribution in the point process breaks into ever larger and more monospecific patches as α approaches one, the effective level of between-patch coupling progressively decreases, ultimately causing dynamics analogous to those in the pseudospatial model with very low m's. Explicit space brings with it the potential for self-organization of a loosely coupled metapopulation.

CONCLUSIONS

Three primary results emerge from out analysis of the moment equations: (1) With finite dispersal and spatially local interactions, α^{CSI} is a humped function of α. The hump moves

to the right as the scales of competition and dispersal increase. As a result, strong competition at the individual level leads to weak competition at the community level. This phenomenon is caused by an ecological analogue of genetic drift. As α approaches one, the deterministic forces opposing stochastic ecological drift decrease, and the tendency of either species to drift to local extinction (or fixation) increases, which gives distinct patches of each species. It is important to understand that the depression of community-level competition by this mechanism is potentially large relative to more widely recognized mechanisms. (2) Because α^{CSI} decreases as M decreases, short scales reduce community-level competition. Small competitive neighborhoods reduce competition because they facilitate the stochastic drift that leads to spatial segregation. Short dispersal further isolates local regions from one another and reinforces drift. (3) Interspecific spatial segregation can cause coexistence. In contrast to the advantages of long dispersal in fugitive-species models (e.g., Levins and Culver 1971), short dispersal facilitates persistence if a species' tendency to segregate exceeds its tendency to aggregate (condition 9.10).

Three independent lines of evidence provide empirical support for some of the above phenomena. First, spatial segregation is nearly ubiquitous and easy to observe. In any place where multispecies vegetation can be viewed from above, count individuals of a species close to randomly selected points (e.g., within a circle with radius equal to canopy height) and then close to randomly selected individuals of another species. A first estimate that is $(1 - b)\%$ of the second implies approximately a $b\%$ reduction in the strength of competition (if the neighborhood radius used is appropriate). If you try this, you will commonly observe biases in excess of 50%. Second, in three of four instances, observed levels of local spatial segregation were shown to have a large effect on community-level competition in field-calibrated models (yes in Pacala and Deutschman 1996; Cain et al. 1995; and Rees, Grubb, and Kelly 1996; no in Pacala and Silander 1990). Moreover, spatial segregation arises spontaneously in data-defined models (see Pacala et al. 1996; Pacala and Deutschman 1996). Third, as reported in Pacala (1996), Kelly and Tripler (unpublished) reviewed over

three hundred published experimental field slides of competition. They found that plant-centered experiments in which neighbors were removed from quadrants centered on focal plants reported statistically significant competition at nearly three times the rate of experiments in which plots were established without reference to the locations of plants (72% versus 26% of experiments showed competition, respectively). Apparently, the fine-scale spatial segregation present in the plot-centered experiments but not in the plant-centered experiments caused the threefold reduction in the interspecific competition detected.

Obviously, the above evidence for the causes and consequences of spatial segregation is incomplete. Experiments are needed to test our four theoretical results against alternative hypotheses. The most likely alternative hypothesis is that habitats are spatially heterogeneous at fine scales and that species coexist and segregate, not because of finite dispersal and local interactions alone, but because each species is the dominant competitor in a different habitat type. One particularly worthwhile experiment would be to transplant plants from a natural community: (1) to a new location with scrambled spatial structure, (2) to a new location with preserved spatial structure, (3) to the same location with scrambled spatial structure, and (4) to the same location with preserved spatial structure (obviously with replicates). Comparisons of the resulting dynamics in 1 and 3 against 2 and 4 would show the importance of fine-scale spatial structure, whereas comparison of 1, 2, and 3 against 4 would test the alternative hypothesis of physically heterogeneous habitat. By following the treatments through time, one could also observe the dynamics of spatial pattern to gain further insight into the genesis of spatial segregation.

The methods presented here allow one to derive the macroscopic population dynamic equations implied by measurable microscopic rules governing births, deaths, and movement by individuals. These methods may be applied to models of virtually any ecological interaction. They promise to close the gap in the current explanatory theory containing the causes and consequences of biologically generated heterogeneity.

ACKNOWLEDGMENTS

We gratefully acknowledge the support of the Mellon Foundation, NASA (NAGW-3741, NAGW-468), the NSF (DEB-9221097), and the DOE (DE-FG04-94ER61815).

APPENDIX

Derivation of the Moment Equations 9.6

Let the random variable q_{it} be the number of species i individuals within a patch. By definition N_i is the mean of q_{it}, σ_i^2 is the variance, and C is the covariance between q_{1t} and q_{2t}.

During the small time interval Δt, q_{it} will change by the amount -1 with probability $\mu_i q_{it} \Delta t$ and by the amount $+1$ with probability:

$$\left[q_{it}(1 - m_i)F(q_{it}, q_{jt}) + m_i \overline{n_i F_i}\right] \Delta t$$

where

$$F(q_{it}, q_{jt}) = f_i - \beta_i q_{it} - \alpha_{ij} \beta_i q_{jt},$$

$\overline{n_i F_i}$ is defined by Equation 9.4.

If we define the operator $E[\ ]$ as the expectation over the "ensemble" of all possible realizations of the model, then

$$E[\Delta q_{it}] = E\Big[(-1)(\mu_i q_{it})\Delta t + (+1)\big((1 - m_i)q_{it}F_i(q_{it}, q_{jt}) + m_i E\left[q_{it}F_i(q_{it}, q_{jt})\right]\big)\Delta t\Big].$$

The expression inside the brackets on the right-hand side is the expected change during Δt given the values of q_{it} and q_{jt} (the sum over all possible kinds of changes of the amount of the change times the probability of the change). The expectation of this conditional expectation over all possible values of q_{it} and q_{jt} (with the operator $E[\ ]$) gives the total mean change.

Using the facts that $E[q_{ii}] = N_i$, $E[q_{ii}^2] = \sigma_i^2 + N_i^2$, and $E[q_{ii}q_{ij}] = C + N_iN_j$ we have

$$\frac{\Delta N_i}{\Delta t} = \mu_i N_i + N_i f_i - \beta_i(\sigma_i^2 + N_i^2) - \alpha_{ij}\beta_i(C + N_iN_j). \tag{9.A1}$$

After taking the limit as $\Delta t \to 0$, we have the first equation in Equations 9.6.

Turning now to the variance σ_i^2, if an individual dies in a patch then q_{ii}^2 changes by an amount $-2q_{ii} + 1$. Similarly, if an individual recruits into the patch then q_{ii}^2 changes by an amount $2q_{ii} + 1$. Thus we have

$$\begin{aligned} E[\Delta q_i^2] = E\Big[&(-2q_{ii} + 1)(q_{ii}\mu_i)\,\Delta t \\ &+ (2q_{ii} + 1)\big(q_{ii}(1 - m_i)F_i(q_{ii}, q_{ij}) \\ &+ m_i E\big[q_{ii}F_i(q_{ii}, q_{ij})\big]\big)\,\Delta t\Big]. \end{aligned} \tag{9.A2}$$

Note that $E[\Delta q_i^2] = [q_{i,t+\Delta t}^2 - q_{it}^2] = \Delta\sigma_i^2 + \Delta N_i^2$. Also, to evaluate the right-hand side of Equation 9.A2, we must evaluate $E[q_{ii}^3]$ and $E[q_{ii}^2q_{ij}]$. We label the third moment $E[(q_{ii} - N_i)^3]$ as T_{iii} and the third moment $E[(q_{ii} - N_i)^2(q_{ij} - N_j)]$ as T_{iij}. Using these definitions

$$E[q_{ii}^3] = T_{iii} + 3\sigma_i^2N_i + N_i^3$$

$$E[q_{ii}^2q_{ij}] = T_{iij} + N_i^2N_j + N_j\sigma_i^2 + 2N_iC$$

and

$$\begin{aligned} \frac{\Delta\sigma_i^2}{\Delta t} + \frac{\Delta N_i^2}{\Delta t} = &-2\mu_i(\sigma_i^2 + N_i^2 - N_i) \\ &+ (1 - m_i)\big[f_i(2\sigma_i^2 + 2N_i^2 + N_i) \\ &- \beta_i(2T_{iii} + 6\sigma_i^2N_i + 2N_i^3 + \sigma_i^2 + N_i^2) \\ &- \alpha_{ij}\beta_i\big(2T_{iij} + 2N_i^2N_j + 2N_j\sigma_i^2 \end{aligned}$$

$$\begin{aligned} &+ 4N_iC + N_jN_i + C)\big] \\ &+ m_i\big[f_i(2N_i^2 + N_i) \\ &- \beta_i(2N_i^3 + 2N_i\sigma_i^2 + N_i^2 + \sigma_i^2) \\ &- \alpha_{ij}\beta_i\big(2N_i^2N_j + 2N_iC + N_jN_i + C\big)\big] \end{aligned} \tag{9.A3}$$

Note that $\lim_{\Delta t \to 0} \Delta N_i^2/\Delta t = 2N_i\,dN_i/dt$. Passing to the limit of infinitesimal Δt and collecting like terms yields the second equation in Equations 9.6 plus two additional third moment terms on the right-hand side: $-2\beta_iT_{iii}(1 - m_i)$ and $-2\alpha_{ij}\beta_iT_{iij}(1 - m_i)$.

Proceeding in a precisely analogous way, we evaluate $E[\Delta q_1q_2]$ to produce the third equation in Equations 9.6 plus two additional third-moment terms on the right-hand side: $-[\beta_1(1 - m_1) + \alpha_{21}\beta_2(1 - m_2)]T_{112}$ and $-[\beta_2(1 - m_2) + \alpha_{12}\beta_1(1 - m_1)]T_{221}$.

Now, why can we omit the third moment terms? If m_1 and m_2 both equal one, then the spatial distribution is Poisson (any non-Poisson initial distribution will die away as the plants initially present die; see Pacala and Silander 1985). We Taylor expand the ensemble distribution $P(n_1, n_2)$ about $m_1 = 1$ and $m_2 = 1$, yielding

$$\begin{aligned} P(n_1, n_2) \approx &R(n_1, n_2) + (1 - m_1)W(n_1, n_2) \\ &+ (1 - m_2)Z(n_1, n_2) \end{aligned}$$

where $R(n_1, n_2)$ is the bivariate Poisson distribution and $W(\ )$ and $Z(\ )$ do not depend on m_1 or m_2. Let T_{iii}^R and T_{iij}^R signify third moments of the Poisson distribution $R(n_1, n_2)$; $T_{iii}^R = N_i$ and $T_{iij}^R = 0$. Thus, the first third moment term above is

$$-2\beta_i(1 - m_i)T_{iii} \approx -2\beta_i(1 - m_i)N_i + O[(1 - m)^2]$$

where $O[(1 - m_i)^2]$ means of order $(1 - m_i)^2$ or $(1 - m_1)(1 - m_2)$, and the remaining three third moment terms above are simply $O[(1 - m)^2]$. We take m_1 and m_2 to be sufficiently close to one that $O[(1 - m)^2]$ terms are negligible. This leaves us with $-2\beta(1 - m_i)N_i$ in the equation for σ_i^2 as the sole remaining third moment term. One could analyze the model with this term included. However, if the average number of individuals per patch is large, then this term is negligible relative to other terms in the second equation in Equations 9.6 (e.g., the terms of order N_i^2, N_iN_j, σ_i^2, $(1 - m_i)N_i\sigma_i^2$, and $(1 - m_i)N_j\sigma_j^2$).

Literature Cited

Atkinson, W.D. and B. Shorrocks. 1981. Competition on a divided and ephemeral resource: a simulation model. Journal of Animal Ecology **50**:461-471.

Bolker, B. and S.W. Pacala. 1996. Understanding the ecological implications of spatial pattern formation using ensemble models. Theoretical Population Biology. Submitted.

Cain, M.L., S.W. Pacala, J.A. Silander Jr. and M.J. Fortin. 1995. Neighborhood models of clonal growth in the white clover, Trifolium repens. American Naturalist **145**:888-917.

Chesson, P.L. 1983. Coexistence of competitors in a stochastic environment: the storage effect. Pages 188-198 *in* H.H. Freedman and C. Strobeck, editors. Population Biology. Lecture notes in biomathematics 52. Springer, New York,

Crawley, M.J. and R.M. May. 1987. Population dynamics and plant community structure: competition between annuals and perennials. Journal of Theoretical Biology **125**:475-489.

Durrett, R., and S.A. Levin. 1994a. The importance of being discrete (and spatial). Theoretical Population Biology **46**:363-394.

Durrett, R., and S.A. Levin. 1994b. Stochastic spatial models: a user's guide to ecological applications. Philosophical Transactions of the Royal Society of London B **343**:329-350.

Gurevitch, J. 1992. A meta-analysis of competition in field experiments. The American Naturalist **140**:539-572.

Hassell, M.P. and R.M. May. 1988. Spatial heterogeneity and the dynamics of parasitoid-host systems. Annales Zoologici Fennici **25**:55-61.

Hastings, A. 1980. Disturbance coexistence, history, and competition for space. Theoretical Population Biology **18**:363-373.

Horn, H.S. and R.H. MacArthur. 1972. Competition among fugitive species in a harlequin environment. Ecology **53**:749-752.

Ives, A.R. and R.M. May. 1985. Competition within and between species in a patchy environment: relations between microscopic and macroscopic models. Journal of Theoretical Biology **115**:65-92.

Levins, R. and D. Culver. 1971. Regional coexistence of species and competition between rare species. Proceedings of the National Academy of Sciences (USA) **86**:1246-1248.

Pacala, S.W. 1996. Models of plant coesistence. *In* M.C. Crawley, editor. Plant Ecology. 2nd Edition. Blackwell Scientific, UK. To appear.

Pacala, S.W., C.D. Canham and J.A. Silander. 1993. Forest models defined by field measurements: I. The design of a northeastern forest simulatior. Canadian Journal of Forestry **23**:1980-1988.

Pacala, S.W., C.D. Canham. J. Saponara, J.A. Silander, R.K. Kobe, and E. Ribbens. 1996a. Forest models defined by field measurements: II. Estimation, error analysis and dynamics. Ecological Monographs **66**:1-43.

Pacala, A.W. and D.J. Deutschman. 1996. Details that matter: the spatial distribution of individual trees maintains forest ecosystem function. OIKOS **74**:357-365.

Pacala, S.W., D. Deutschman, C. Canham and J. Saponara. 1996b. Interspecific tradeoffs and the maintenance of biodiversity in a north temperate forest. Ecological Monographs. Submitted.

Pacala, S.W. and J.A. Silander, Jr. 1985. Neighborhood models of plant population dynamics. I. Single-species models of annuals. The American Naturalist **125**:385-411.

Pacala, S.W. and J.A. Silander, Jr. 1990. Field tests of neighborhood population dynamic models of two annual weed species. Ecological Monographs **60**:113-134.

Pacala, S.W. and D. Tilman. 1994. Limiting similarity in mechanistic and spatial models of plant competition in heterogeneous environments. The American Naturalist **143**:222-257.

Rees, Mark, P.J. Grubb and D. Kelly. 1966. Quantifying the impact of competition and spatial heterogeneity on the structure and dynamics of a four-species guild of winter annuals. The American Naturalist **147**:1-32.

Shmida, A. and S.Ellner. 1984. Coesistence of plant species with similar niches. Vegetation **58**:29-55.

Skellam, J.G. 1951. Random dispersal in theoretical populations. Biometrika **38**:196-218.

Tilman, D. 1982. Resource competition and community structure. Princeton University Press, Princeton, NJ, USA.

Tilman, D. 1994. Competition and biodiversity in spatially structured habitats. Ecology **75**:2-16.